Section A-Research paper

MAGNETICALLY ADSORPTION OF COPPER REMOVAL FROM INDUSTRIAL WASTE WATER USING NANOCOMPOSITES

G.Mohankumar[1]*, S.Sathian[2], P.Akilamudhan[3], and A.Murugesan[4]

[1*,2]Department of Chemical Engineering, Annamalai University,
Annamalai Nagar, Chidambaram, Tamilnadu-608002, India
[3]Department of Chemical Engineering, Erode Sengunthar Engineering College
(Autonomous), Erode, Tamilnadu-637 205, India
[4]Department of Chemical Engineering, Nandha Engineering College (Autonomous),
Erode, Tamilnadu-638052, India

ABSTRACT

Feasible reutilization of Fe3O4/MnO2 Magnetic sorbents were recycle utilized to remove Cu (II) from industrial wastewater. In this paper, The Fe3O4/MnO2 composites structure and interface adsorption mechanism were investigated by chemical affinity, zero potentials combining with XRD, FTIR and TEM. The adsorption, desorption and recycle experiments were explored. The results indicated that Fe3O4/MnO2 composites were nano structure with consisting of two layers with Fe3O4 in the core and amorphous MnO2 on the shell. The adsorption mechanism was that the heavy metals substituting for H of Mn–O–H and forming the structure of Mn–O–Me which meant the metals removal was the process of ion exchange. The sorbent removal efficiency of Cu, were 99.76% respectively. The equilibrium data analysis indicated that the Langmuir model was the most appropriate model to describe the adsorption of on the surface of Fe3O4/MnO2 composites. The kinetics studies showed that the adsorption kinetics of heavy metal ions on the surface of Fe3O4/MnO2 composites was significantly appropriate to pseudo-second-order model. The experiments verified that the Fe3O4/MnO2 sorbent being separated from water by external magnetic field for recycling was feasible for environmentally friendly and efficient remove heavy metal ions.

Key words; Cu (II), Fe3O4/MnO2 sorbent, industrial waste water, Langmuir model.

[1]* *Corresponding author* : *G.Mohankumar*

E-Mail address : petromohankumar@gmail.com (G.Mohankumar)

Mobile Number : 9942498882

Introduction

Contamination of soils and sediments with trace metals was worldwide problem originating from many industrial activities, such as ore processing, printing, metallurgy, batteries, electroplating, mining and chemical [1,2]. Heavy metal ions such as Pb, Cu, Cd and Zn were among the most common pollutants in industrial effluents [3,4] which did harm to human health and other living organisms. Consequently, Research had focused on the removal of metal ions contaminants to acceptable level of environmentally friendly. In recent years, various methods for heavy metal removal from wastewater had been extensively studied. Various approaches, such as chemical precipitation, electrochemical treatment, ion exchange and adsorption, had been proposed to remove heavy metal ions from contaminated water [5,6]. Among these methods, adsorption was an attractive approach in contaminated water treatment, due to its high removal efficiency reliability, economy and without yielding harmful by-products [7].

Recently numerous approaches had been studied for the development of cheaper and more effective mineral adsorbents. Minerals had been increased attention for heavy metals remediation applications for high sorption capabilities for metal [8,9]. Particularly, the nanostructure mineral offering large surface areas, which provided high capacity and the ability to enhance contaminant affinity with the surface [10,11]. Therefore, MnO2 had been chosen to prepare composited sorbents to adsorb heavy metals [12]. Unfortunately, such minerals still suffered from issues involving inconvenience of separation from the waste water as they tended to form super fine particles in aqueous solution and cause secondary pollution. Thus, the development of new Nano sorbents with a facile separation property and recycling utility was of great interest. Iron oxide like magnetite (Fe3O4) and maghemite (γ-Fe2O3), had been extensively applied in designing because they had a high magnetic susceptibility. The modification of Fe3O4 with MnO2 was not only removal heavy metal ions efficiently but also recovery through its magnetic property.

The adsorption was found to be accomplished by surface complexation. There was a lack of knowledge about the surface structure-sensitive adsorption and adsorption mechanism. How the parameter impact on heavy metals adsorption, and the adsorbs worked efficiency after times recycle were still not clear. In this paper, the Fe3O4/MnO2 composites were used as cyclic sorbent to remove the heavy metals ions such as Cu (II), from industrial wastewater. The surface structure and property of Fe3O4/MnO2 composites were characterized. The influent parameters of remove heavy metals from waste water were investigated. Chemical affinity and total capacity of the composites were shown to be superior to select heavy metals in the wastewater. The surface adsorption isotherm and kinetics of Fe3O4/MnO2 composites were investigated. The adsorption and desorption

and the recycle remove of heavy metals were explored. The removal heavy metals mechanisms of Fe3O4/MnO2 composites sorbent were elucidated.

2. Experimental sections

2.1 Synthesis of magnetic Fe3O4/MnO2 composite

The magnetic composites Fe3O4/MnO2 were prepared with a simple hydrothermal process on the basis of previous literature reports [13], and the modifications was needed in this experiment. During the synthesis process, 0.51 g KMnO4 was first dissolved in 35 mL of deionized water. 0.8 mL HCl (37 wt%) was slowly added to the solution and stirred for 30 min. Then 0.32 g Fe3O4 was added into the solution and stirred continuous for 1 h. The mixture was washed with deionized water, and then dried at 120 °C for 2 h under atmospheric conditions.

2.2 Characterization of magnetic Fe3O4/MnO2 composites

The morphology of the products were examined by field-emission scanning electron microscopy (SEM) and transmission electron microscopy (TEM). Crystalline phases were identified by X-ray diffraction (XRD). Magnetic property measurement was performed on vibrating sample magnetometer (VSM). Surface area and pore size distribution were measured by the Brunauer–Emmett–Teller (BET). The zeta potentials were measured with a zetasizer. In order to obtain information about the distribution of metals ion within the Fe3O4/MnO2 nano-composites, the samples were immerged with waste water for 24 h. The interaction between heavy metal ions and the adsorbent were examined by FTIR. The elemental compositions were determined by EDX and inductively coupled plasma atomic emission spectrometry (ICP). The pH PZC (point of zero charge) of composites was defined as the pH value at which the surface carries net zero charge. To evaluate the pH PZC, the acid and base titrations were carried out, and the corresponding pH was recorded using a pH meter.

2.3 Experiment of recycle removes Cu (II) from waste water

Industrial waste water contained heavy metals Cu (II) with the concentration of 10 mg L−1 of each metal. The magnetic Fe3O4/MnO2 composite were applied as sorbent to remove heavy metals from industrial waste water. Fe3O4/MnO2 composites sorbent was placed into the waste water and shaken for 24 h on a rolling mixer (20 rpm). The remove heavy metals experiments were performed at pH ranging from 2 to 12 and temperature ranging from 30 to 60 °C. The composites sorbent was then collected from the solution using a NdFeB magnet. The waste water (after remove the heavy metals) was analysed by inductively coupled plasma atomic emission spectrometry (ICP). Each batch experiment was repeated thrice and the relative error was found to be within ± 2%, and the final data were the average values.

The removal degree was estimated by the capacity of removal heavy metals in solution before and after adsorption, the formulas were shown as follow:[14]

$$qe = (Co-Ce)/ (Co) \quad (1)$$

Where qe (%) was removal degree, Co and Ce (mg L−1) were the initial and final metals concentrations in the solution, respectively.

For the desorption experiment, Fe3O4/MnO2 loading heavy metal ions was dipped into 0.1 M HCl solution, the mixture solution was stirred continuously in a shaker for 0.5 h at 30 °C. The composites sorbent was then collected with a NdFeB magnet and then concentrations of metal ions in the solution were analysed. Fe3O4/MnO2 composites was used in the next adsorption cycle after washing and drying. The quantity of ions desorption per unit mass of used adsorbent were calculated according to the following equations:

$$qde = CV0 /m_O \times 100 \quad (2)$$

While qde (%) was desorption degree (%), C was the metal ion concentrations in the desorption solution (mg L−1), V0 is the volume of the desorption solution (L), m0 was the heavy metal ions amount in before desorption (mg).

2.4 Adsorption isotherms

Langmuir and Freundlich models were the usual models for investigating the adsorption isotherms [15, 16]. Langmuir adsorption isotherm offered the homogeneous adsorption activation energy of adsorbent and envaulted the maximum adsorption capacity. Furthermore, this isotherm presumed monolayer adsorption. The linear form for the Langmuir isotherm model was expressed as Eq. (3). Freundlich isotherm described both monolayer and multilayer adsorptions. Freundlich isotherms were often used to describe adsorption equilibria between solid and solution. The linear form for the Freundlich isotherm model is expressed as Eq. (3) and (4):

Langmuir adsorption isotherm; $Ce / qe = 1 / kqm + Ce / qm$ (3)

Freundlich isotherm; $logqe = logk' + 1 / n \log Ce$ (4)

where the Ce and qe were the equilibrium concentration of heavy metal ions (mol L−1) and the amount of heavy metal ions adsorption on the mineral at equilibrium (mg g−1), respectively. k was the Langmuir isotherm constant, and qm was the maximum monolayer coverage capacities (mg g−1), n was related to adsorption capacity and k′ was the Freundlich isotherm constant (mg g−1) (L mg−1).

2.5 Adsorption kinetics

Study of the adsorption kinetics provided the rate of adsorbed heavy metal ions on the surface of sorbent. Pseudo-first and pseudo second order models were the most common kinetic models used for modelling the kinetic rates [17]. These models were also estimated the amount of adsorbed heavy metals on the surface of sorbent at various time intervals. The equations of these models can be expressed as follow.

The pseudo first order kinetic equation was represented by Eq. (5).

$$\ln (qe - qt) = \ln qe - kLt \quad (5)$$

The pseudo second order (PSO) kinetic equation was represented by Eq. (6).

$$t/qt = 1/kq2e + 1/qe \times t \quad (6)$$

where qe and qt was the heavy ions adsorption quantity (mg g−1) at equilibrium time and time t, respectively, kL and k were the rate constants of pseudo-first and second order models, respectively. qt had exponential relation with t in the pseudo-first-order model while the relation between t/qt and t was linear for the pseudo-second-order model.

Results and Discussion

Phase –geometry identification

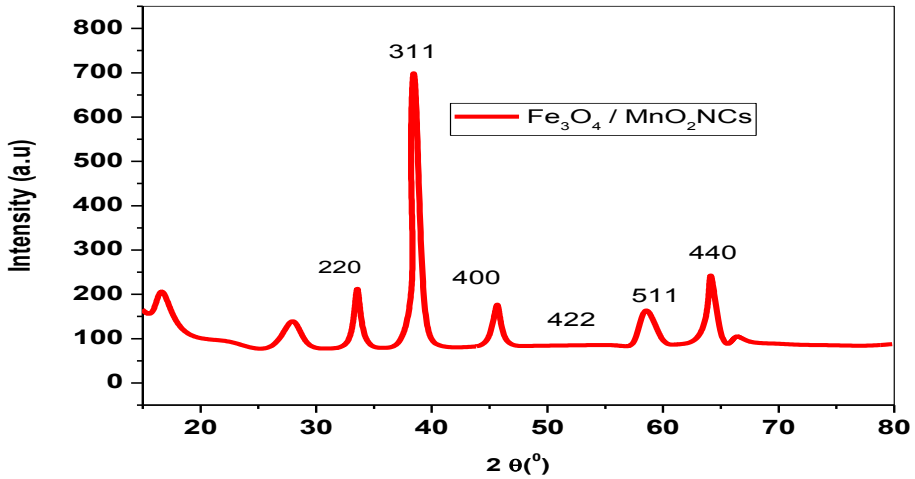

Fig. 1. The phase structure of composites particles was characterized with XRD

The patterns of Fe3O4/MnO2 composites were similar with that of Fe3O4, but the peaks strength of Fe3O4/MnO2 composites were weaker compared with that of Fe3O4. In addition, all the diffraction peaks were identified to face-centred cubic crystal of Fe3O4 (space group: Fd3m, a = b = c = 8.394 A). No visible MnO2 crystalline peaks were detected in all lines, which inferred that out shell MnO2 was amorphous phase.

Topological analysis

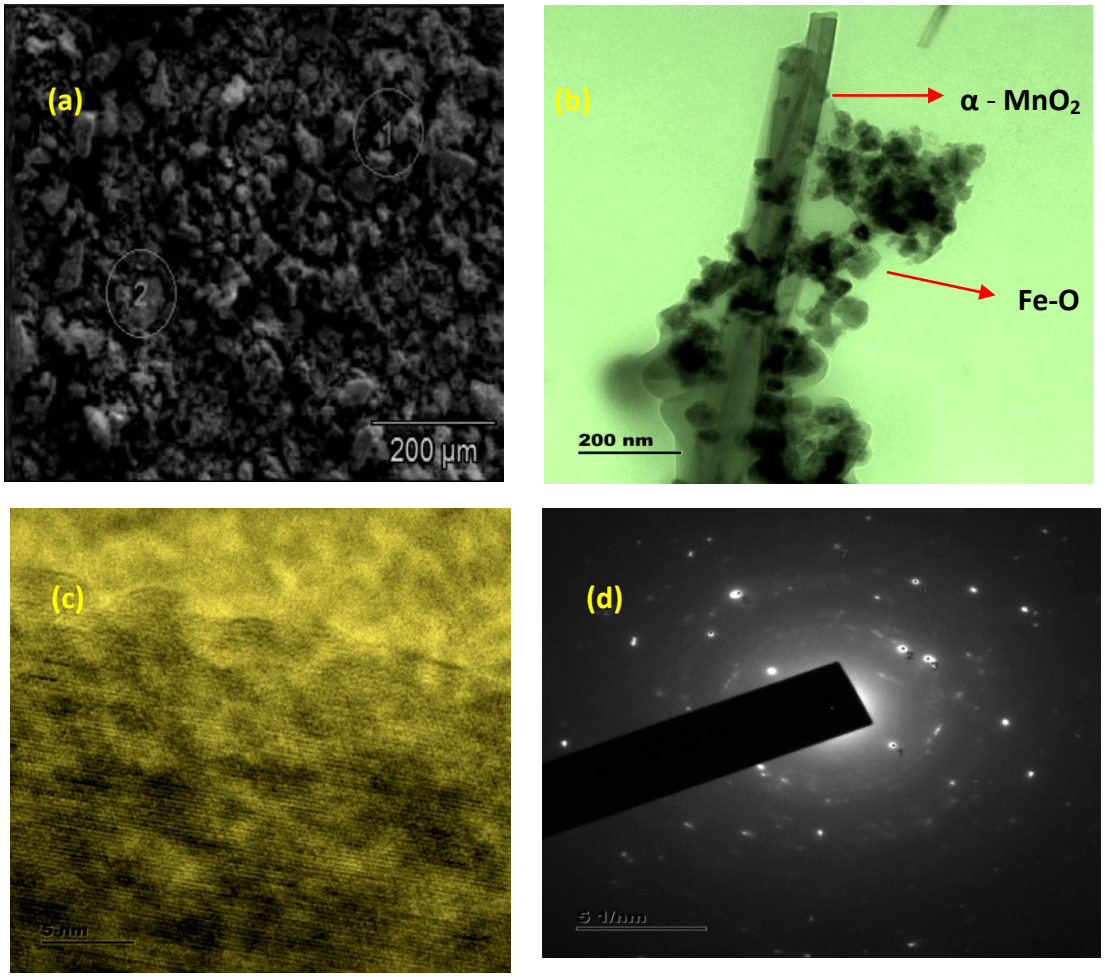

Fig-2(a) SEM image of Fe_3O_4@MnO_2 (b) TEM microscopic spectrum of Fe_3O_4@MnO_2 NRs (c) HR-TEM image of Fe_3O_4@MnO_2 (d) SAED pattern of Fe_3O_4@MnO_2 NCs

[Fig- 2 (a)] shows the structural and morphological spectrum of Fe3O4@MnO2 NCs. These SEM images showed granular shapes with no assemblage and un equality of homogeneously Fe3O4@MnO2 NCs. Figures 2 (c) HRTEM shows the surface characteristics of Fe3O4@MnO2 NCs. [Fig-2 (b)] shows that TEM images of Fe3O4@MnO2 NCs indicate rod like spherical in patterns with molecule size varying from 12 to 22 nm. Furthermore, the monocrystalline phase of Fe3O4@MnO2 NCs by co-precipitation strategy was supported by their corresponding SAED examination, as shown in Fig.2(d), with recognizable peak (311), (400), (422), (511) and (400) crystallographic patterns recommending cubical symmetric spinel strategy. The HR-TEM illustration also reveals a well inner surface of the ligament, with the d –widths for adjoining interlayer fringes one assessed to be 0.236 nm, that also represents the proportion of the (311) plane cubical symmetric spinel of Fe3O4@MnO2 NCs [18, 19]

Vibrational spectrum analysis

Infrared spectrum was operated to analysis the spectrums of the sorbent Fe3O4/MnO2 nano-composites, ferro ferric oxide and manganese dioxide. The infrared scanning range was 400 - 4000 cm−1. Referred to the standard infrared spectrum of ferro ferric oxide and manganese dioxide, the absorption peaks at 584 cm−1 were the Fe–O characteristic absorption peak and peak at 3400 cm−1 was stretching vibration of hydroxy ferric iron. The infrared absorption peaks at 3400 cm−1, 1625 cm−1, 1348 cm−1, 553 cm−1 were infrared characteristic peaks of manganese dioxide. And the peak at 3400 cm−1 was the surface hydroxyl stretching vibration peak of Mn–O, the peak at 1625 cm−1 was the stretching vibration peak of the combination of Mn–O and O–H. As shown in Fig. 3, the absorption peaks of Fe3O4/MnO2 composites happened at the characteristic absorption peaks of ferroferricoxide and manganese dioxide, which proved that this nano-composites sorbent was a composite product of Fe3O4 and MnO2. [20-22]

3.4 BET isotherm of Fe3O4@MnO2NCs

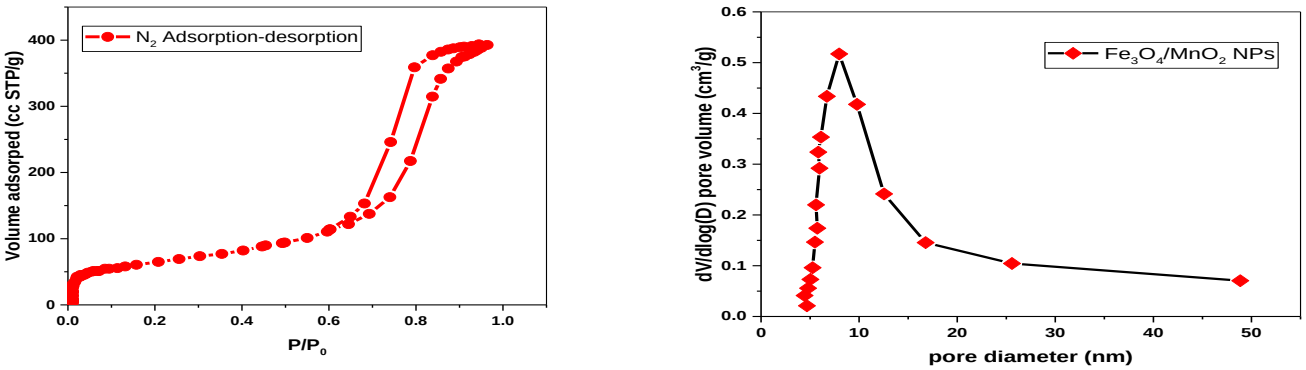

Fig- 3 (a) N2 adsorption-desorption isotherms (b) pore volume vs pore diameter of Fe3O4/MnO2 NCs

The N2 adsorption-desorption isotherm models and pore size diffusion of a novel Fe3O4@MnO2 impetus are displayed in Fig 3 (a & b). Figure 3 (a) illustrates an impressively genuine MnO2@Fe3O4 impetus with a group IV isotherm, which emerges to be a characteristic revealed by hierarchical highly permeable components. The inter - facial state (SBET) was assessed using Brunauer–Emmett–Teller (BET) approach, and the pore diameter correspondence was acquired utilising the Barrett–Joyner–Halenda (BJH) tactic case and even the adsorption isotherm band. Figure 3 (b) demonstrates how the volume immobilized rapidly with increasing comparative imperative attributes for all isotherms depending on the volume required to fill of mesopores in Fe3O4 screenplay. The porosity and surface province of MnO2@Fe3O4 and the permeability length across were characterised to be 13.19 m2/g and 0.059 cm3/g, respectively [23, 24].

3.5 EDX spectrum and Elemental mapping Analysis

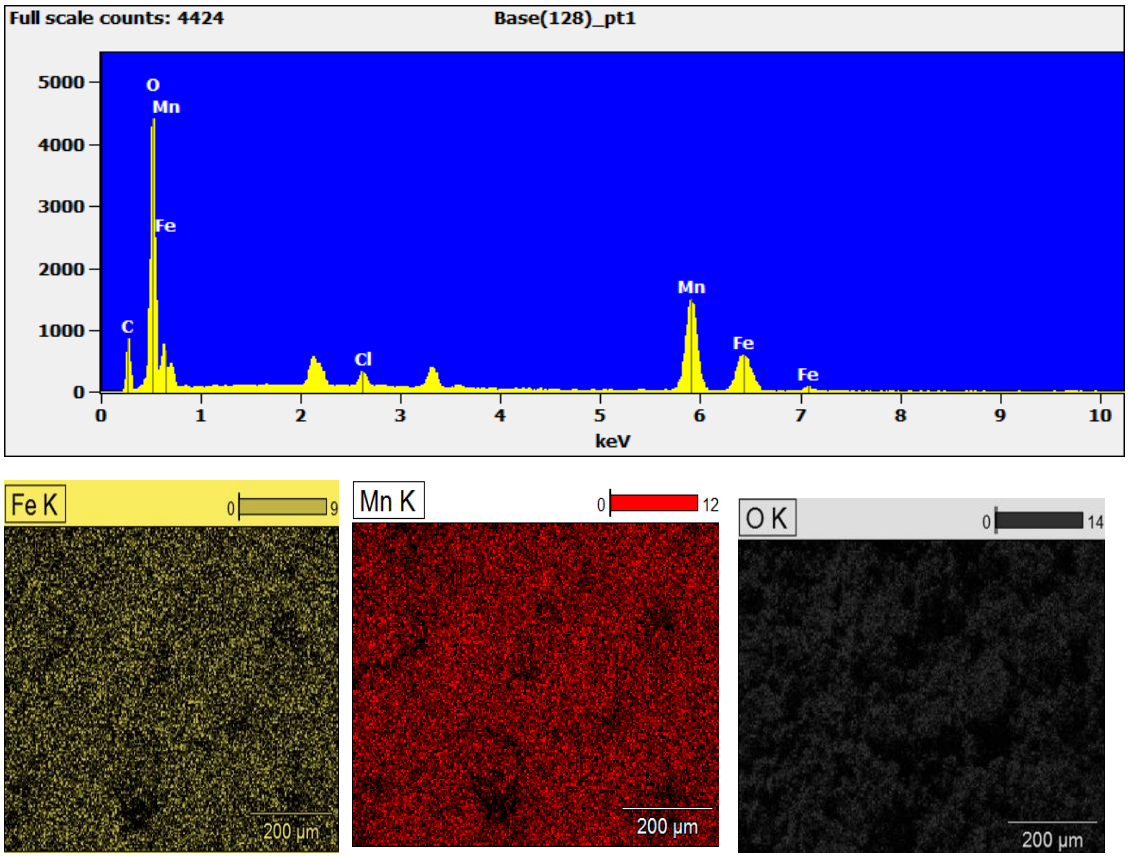

Fig-4 (a)Energy Dispersive Spectroscopy (b) Elemental Mapping spectrum

Elemental analysis of Fe3O4@MnO2 NCs photo detectors demonstrated that certain components, chiefly iron, oxygen, and Mn were generally provided in the hybrid Fe3O4@MnO2 nanocomposite. Moreover, the EDX template of Fe3O4@MnO2 NCs reported the existence of all component parts including such Fe, O, and Mn were shown in Fig – 4 [25]

3.6 AFM analysis

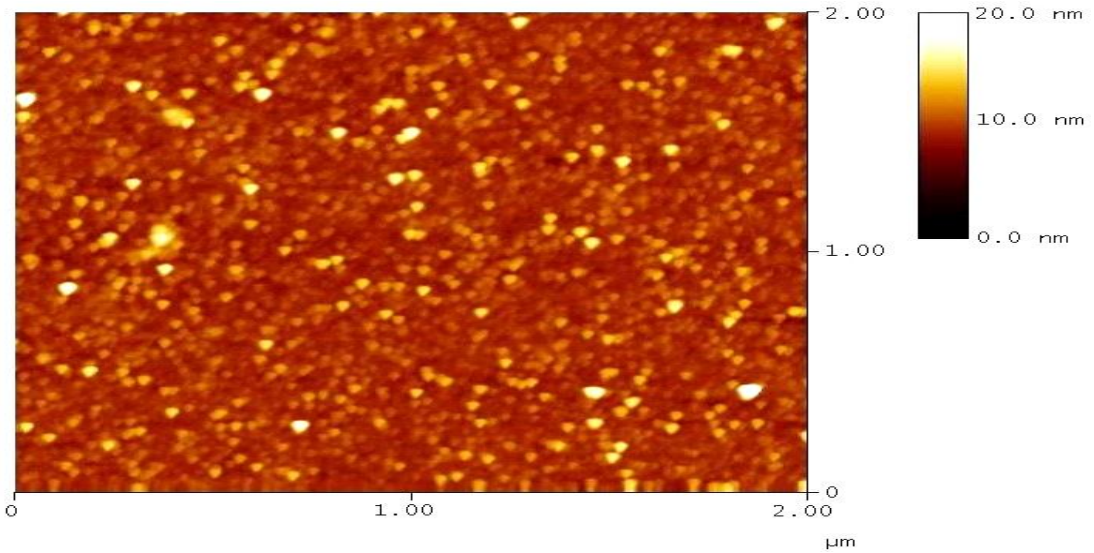

Fig-5. Atomic force microscopy of synthesized Fe3O4/MnO2 NCs

The AFM is a type of electron microscopy that is being used to detect factors like length. In tapping phase, an AFM image of Fe3O4/MnO2 was captured. Surface morphology, which is commonly expressed in dimensions of exterior hardness, is essential for forecasting catalytic characteristics. The root mean square roughness (RMS) of a material is related to its particle diameter. The average rough surface was 5.89 nm, with the Root Mean Square at 10.37 nm. The rougher the texture and the greater the contact area, the more activation centres there are. The excessive annealing temperature [26] may have caused the Nano catalyst's irregular structure.

3.7 Magnetic behaviour of synthesized Fe3O4/MnO2 nanocomposites

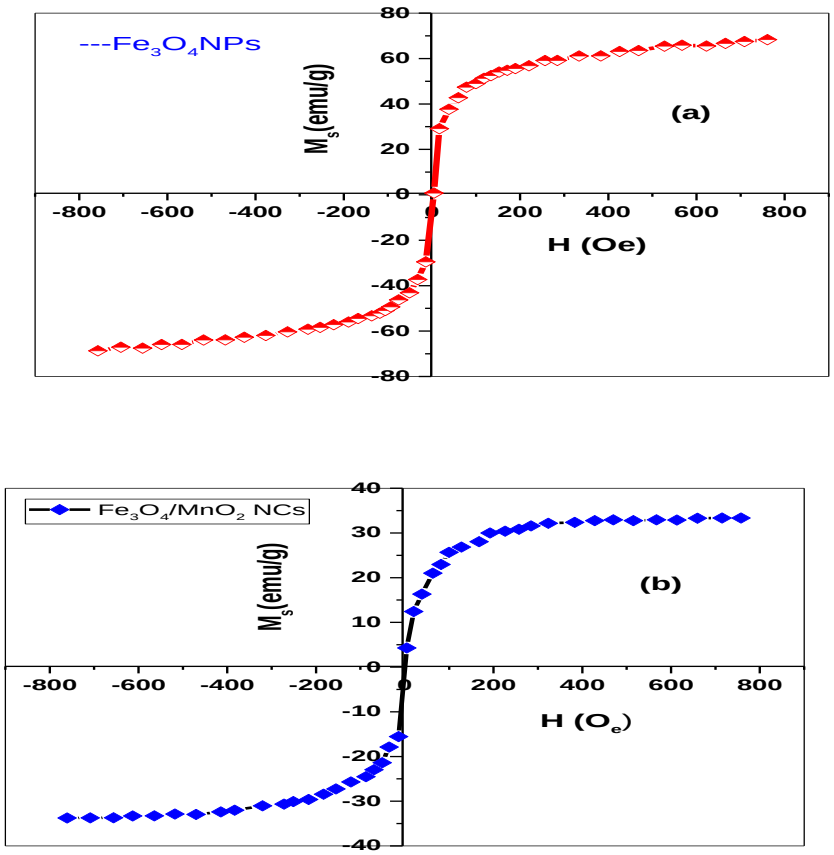

Fig-6 VSM spectra for (a) Fe3O4 (b) Fe3O4/MnO2 nanocomposites by co-precipitation method

The magnetic profiles of Fe3O4 nanoparticles and Fe3O4/MnO2 composite fragments are shown in Figure 6 (a) and (b). Two very different designs are similar, and the Fe3O4/MnO2 composite particles possess super-paramagnetic characteristics. Even as permanent magnet field was curtailed, the ferromagnetism lessened until it dropped to zero at H = 0. No residual magnetic moment stayed. It further inhibits particle aggregation,

and the powders could be incredibly quickly distributed equally because once the magnetic field is excised. Fe3O4 nanoparticles have a saturation magnetization of 68.1 emu/g, while Fe3O4/MnO2 considered as part have a magnetization of 33.5 emu/g. [26,27]

3.8 Adsorption studies

The degrees of remove heavy metals of Fe3O4/MnO2 nano-composites were shown in Fig. 2. The results showed that Fe3O4/MnO2 nano-composites had relatively high adsorption capacity owing to their larger surface area, which contributed to the increase in the number of adsorption sites for the heavy metals. In addition, MnO2 had abundant surface functional groups and high-density negative charges verified before. The removal degrees of the four heavy metal ions Cu were 99.81%, respectively.

Adsorbent dosage

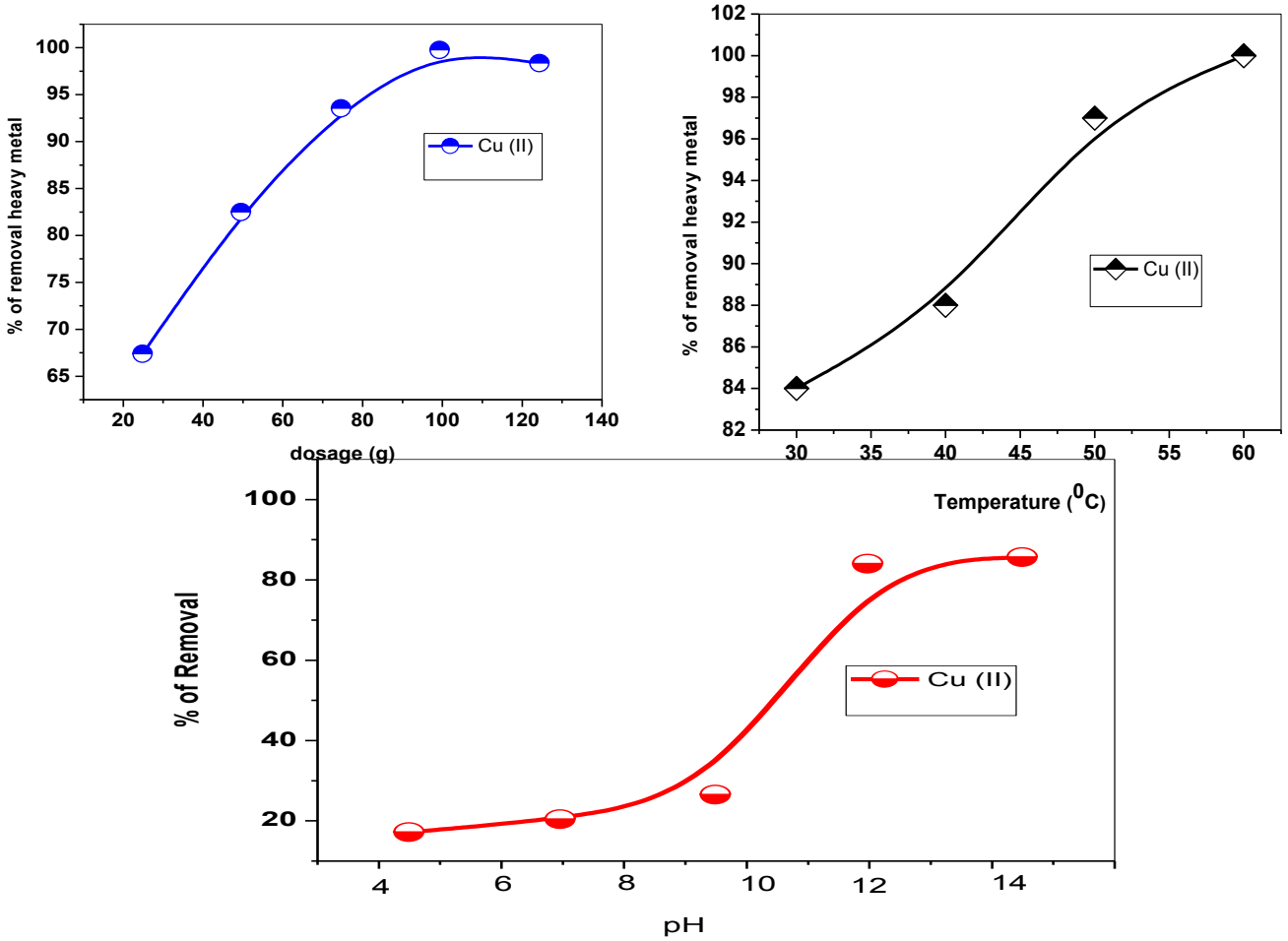

Fig.7. The effect of dosage on Fe3O4/MnO2 nano-composites remove heavy metals

The dosage of sorption for removal heavy metals from waste water was significant for efficiency. The removal of heavy metals from waste water increased obviously with the increase of Fe3O4/MnO2 nano-composites dosage when the dosage was less than 1.0 g L−1. As the Fe3O4/MnO2

nano-composites dosage increased, the number of available sites for binding heavy metal ions increased, which could improve the removal heavy metal ions. When the dosage of Fe3O4/MnO2 nano-composites increased to excess 1.0 g L−1, the mounts of removal heavy metals decreased. The result was that the increase of sorbent dosage could decrease the contact area between metal ions and solid surface. [28, 29]

Effect of temperature

Effect of temperature is a one of the most important parameters in the absorption process. Fig. 7b represents the influence of temperature on the adsorption capacity of Fe3O4/MnO2 nanoparticles in the range of 30-600C at room temperature. As it is shown in Fig. 7b, it is obvious that increasing of temperature results in increasing of Cu (II), removal from aqueous solution. As depicted, adsorption was fast and equilibrium reached after 2h. This rapid adsorption can be attributed to high dispersion of nanoparticles, high external surface area and lack of internal diffusion limitation [30, 31] After the 10 minutes, there was little change in the absorption rate and it reflects that process would reach to the equilibrium state. The optimum temperature for the adsorption using NCs was Fe3O4/MnO2 achieved at 500C.As a result, to ensure complete equilibrium state, all of the experiments were performed for 600C.

Effect of pH

The pH of the watery arrangement might be the main boundary in the adsorption cycle which influences metal particles and surface charge of adsorbent [29, 30] Since at pH>12 the Cu (II), particles begin to hasten, the examinations were done at pH 3–14.[32] As found in Fig. 7c, expanding pH brings about expanding adsorption limit from 68.55 to 108.58 mg/g. The justification for this outcome is that higher pH lead to more deprotonation of adsorbent surface that, expands negative charged locales, which is favour for electrostatic fascination between surface of adsorbent Cd (II), consequently builds the adsorption limit. While, lower pH lead to all the more decidedly charged destinations, which expands shock powers between adsorbent surface Cu (II), particles that diminishes the adsorption limit [31] Thus, pH 10-12 was considered for additional tests.

3.9 Isotherms models

Adsorption isotherms were used to achieve more information about the adsorption behaviour and adsorption parameters such as the adsorption maximum capacity on the surface of Fe3O4/MnO2. The results of equilibrium data for Cu2+, sorption was presented for Langmuir and Freundlich isotherm in Fig. 8a, b, respectively. As seen from Fig. 8a, the adsorption densities of heavy metal ions for sorbent were improved with increasing the concentration of metal ions, which confirmed that the initial concentration was a driven force for adsorption process.

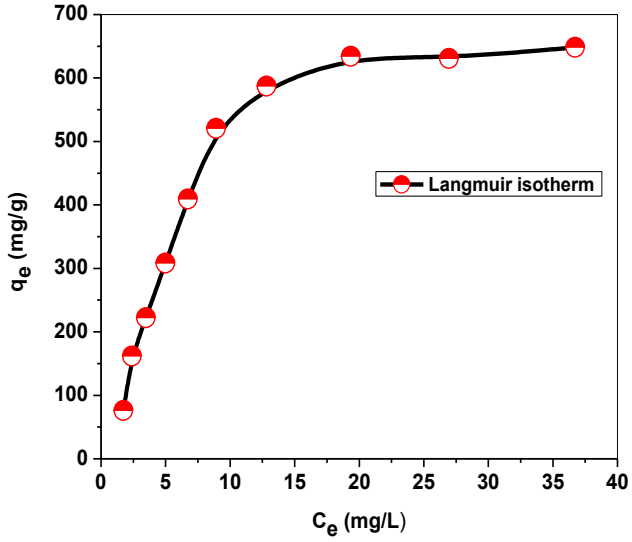
Langmuir isotherm
q_e (mg/g)
C_e (mg/L)

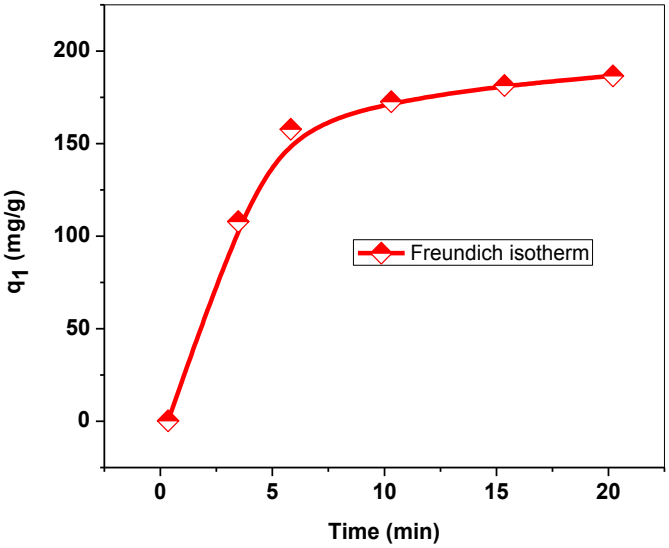
Freundich isotherm
q_1 (mg/g)
Time (min)

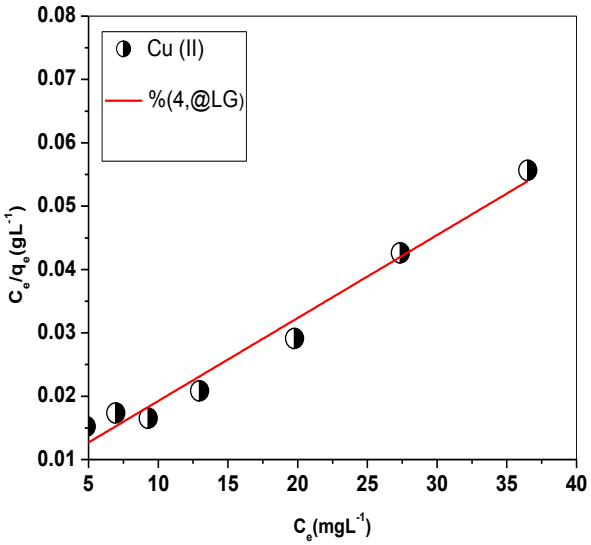
Cu (II)
%(4,@LG)
C_e/q_e (gL^{-1})
C_e(mgL^{-1})

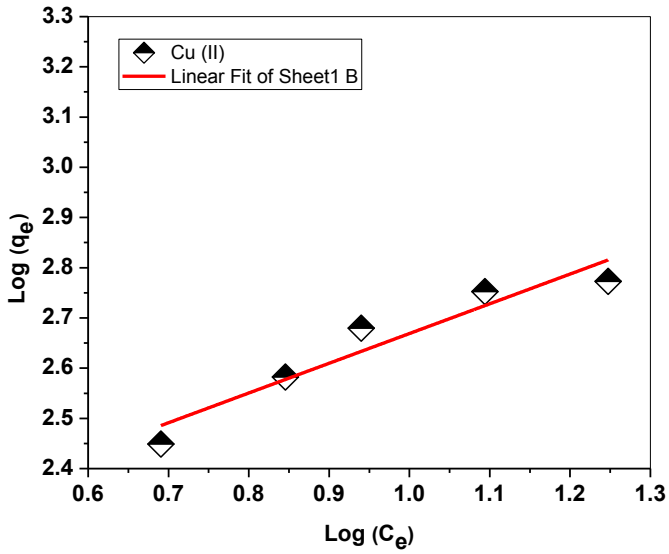
Cu (II)
Linear Fit of Sheet1 B
Log (q_e)
Log (C_e)

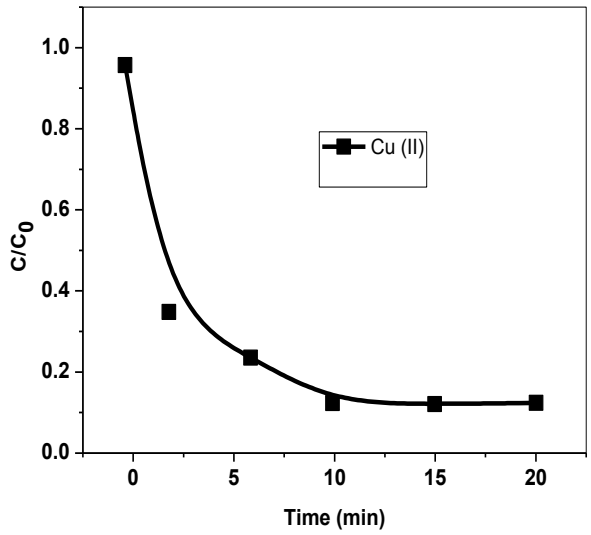
Cu (II)
C/C_0
Time (min)

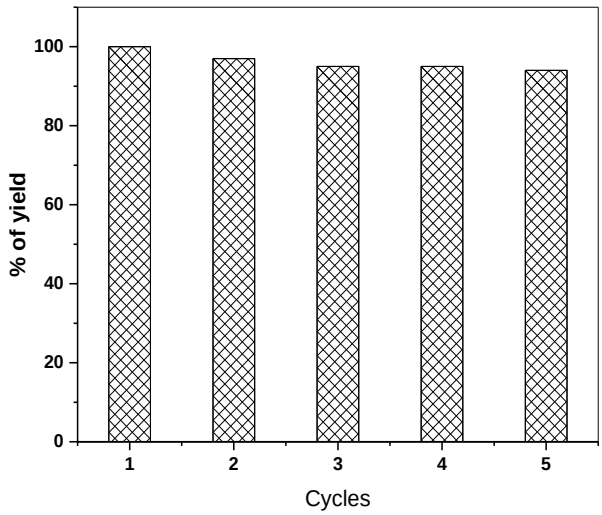
% of yield
Cycles

Fig -8 (a) Experimental maximum Adsorption of isotherm of Cu (II on Fe3O4/MnO2 (b) Experimental maximum Adsorption of capability with time (c) Langmuir isotherm model (d) Freundlich isotherm model (e) kinetic plot (f) reusability of Fe3O4/MnO2 nanoparticles

The results of the two isotherm models as a function of heavy ions concentration at a pH of 6.5 and room temperature were presented in Table 1. The results showed that R2 values of the Langmuir isotherm model was the higher than that of Freundlich isotherm model. Langmuir isotherm model was the best describing model for Cu2+, Cd2+, Zn2+ and Pb2+ adsorption on Fe3O4/MnO2 surface. This model postulates that the monolayer adsorption of metal ions on the Fe3O4/MnO2 surface with all adsorption sites would be formed and being energetically equivalent. All relations between Ce/qe and Ce of heavy metal ions were linear. The correlation coefficient value (R2) except Cd2+ were higher than 0.99. As shown from Table 1, the Maximum adsorption capacity qm value of the Langmuir isotherm model for Fe3O4/MnO2 adsorption Cu2+, was 498 mg g−1, respectively which was much higher than the references [31], which meant MnO2 acted on the adsorption. The metal ions order according to Langmuir model were Cu2+ according to the k values.

Table 1:

Heavy Metal	**Langmuir isotherm**			**Freundlich isotherm**		
CU^{2+}	$q_m(mgg^{-1})$	K	R^2	K’	n	R^2
	568.3	7.92	0.9920	152.3	2.673	0.998

Table 1: Various isotherm models of copper remove from industrial waste water

3.10 Adsorption kinetics

In Adsorption Kinetics, the Fe3O4/MnO2 adsorption heavy ions capacity change with time discussed. The dosage was 1 g L−1, with the initial heavy ion contents of 10 mgL−1, and the temperature of 30 °C. The adsorption capacity qt of Cu2+, in waste water increased to 480 mg g−1, within 100 min. From the slope of the curve, it could deduce that the adsorption rate increased in 100 min, and then slow down during 100min because of adsorption site reducing rapidly.

Similarly the kinetic adsorption parameters which were fitted by pseudo-first and pseudo-second-order models. A relatively higher correlation coefficient R2 values of pseudo-second-order model was the higher than that of pseudo-first model. The pseudo-second-order models described well the adsorption kinetics of heavy metal ions on the surface of Fe3O4/MnO2,

which meant that the rate of adsorption should be proportional to the concentration of metal ions in the solution. Also, the rate of the adsorption was controlled by the chemical the exchange. These results revealed that the surface chemistry of minerals could be changed by surface dissolution.

The Fe3O4/MnO2 composites had high potential to adsorption heavy metal ions after 5 times cycle removing Cu2+, from wastewater. The cycles of adsorption and desorption of the Cu2+ were shown in Fig. 13. The removal efficiency 99.76% for Cu2+ sorption, in latter three times cycles the removal efficiency slightly floating up and down at 99.6%. The removal efficiency increased from 97.55 to 98.62% for Pb2+ sorption, at latter three times cycles, the removal efficiency was up to 98%. For Cu2+, the removal efficiency decreased from 97.8 to 95.7% in the second cycle, but it increased again in the last three cycles, and it could be found that the efficiency remained as high as 99.6% after five cycles. The increase of removal efficiency in the process of recycling might be due to the fact that the large bulks of adsorbent break into small ones, leading more active sites were exposed during the repeated cycles. The adsorption Zn2+ degree of Fe3O4/MnO2 nano-composites was 85% after 5 times recycle.

Table 2: Kinetic Adsorption Parameter

Heavy Metals	**Pseudo First Order**		**Pseudo Second Order**	
	K_L	R^2	K	R^2
CU^{2+}	0.0042	0.9599	0.0386	0.998

Recycle process

The dosage was $1gL^{-1}$ with every inial heavy ion contents of 10 mg L^{-1} and the temperature of 30 °C. The y-axis was split to allow for observation of the differences cycle in the remove of Cd^{2+} for each adsorption/desorption cycle. The arrow tip was added to enhance clarity of the Cd^{2+} adsorption and desorption steps of the cycles, respectively. Initial contact showed almost complete adsorption of Cd2+ (96.5%), followed by nearly complete stripping of the Cd^{2+} by the HCl wash step. The cycle was repeated with Cd^{2+} loading followed by nearly complete removal by the HCl wash step for five cycles with capture efficiencies of 96.5, 99, 98, 99 and 97% Cd for the subsequent cycles. The five times accumulation of Cu2+, Cd2+, Pb2+ remove from water by core–shell structure Fe3O4/MnO2 was over 2375 mg g−1 respectively. The five times accumulation for Zn2+ was 2017.5 mg g−1. The core–shell structure Fe3O4/MnO2 had the performance of adsorption–desorption and provided cost-effective, high efficiency, and magnetically manipulable sorbents which could be enable a range of remediation, recycling, and analytical solutions. [33, 34]

Conclusion

Magnetically Fe3O4/MnO2 nano-adsorption was demonstrated the ability to remove copper from industrial wastewater. The results showed that Fe3O4/MnO2 Core–shell nano-adsorption was a friendly environmentally with higher affinity and capacity to remove copper from water. Thus, the copper ions removal result showed that Fe3O4/MnO2 nano-composites adsorption capacity of copper ions was high and the removal ratios of copper were exceeded 99%. The equilibrium data analysis indicated that the Langmuir model was the most appropriate model to describe the adsorption on the surface of Fe3O4/MnO2 composites. The kinetics studies showed that the adsorption kinetics of heavy metal ions on the surface of the sorbent was significantly appropriate to pseudo-second-order model. The adsorbed metal ions substituted the hydrogen atoms and formed new complex with oxygen in the homologous functional groups. The heavy metals substituted for H formed the structure of Mn–O–Cu, which meant the copper removal was the process of ion exchange. The adsorption of copper ions on Fe3O4/MnO2 nano-composites was dependent on pH and with the dose of sorbent. Recycle times of removal results suggest that magnetic Fe3O4/MnO2 nano-composites could be removed copper ions from wastewater effectively.

References

[1]. Dhir B., Potential of biological materials for removing heavy metals from wastewater. Environ. Sci. Pollut. R., 2014, 21, 1614-1627.

[2]. Abdel-Halim S.H., Shehata A.M., El-Shahat M.F., Removal of lead ions from industrial waste water by different types of natural materials. Water Res., 2003, 37, 1678-1683.

[3]. Barbosa F Jr (2017) Toxicology of metals and metalloids: promising issues for future studies in environmental health and toxicology. J Toxicol Environ Health Part A 80(3):137–144

[4]. Acharya J., Kumar U., Meikap B., Thermodynamic characterization of adsorption of lead (II) ions on activated carbon developed from tamarind wood from aqueous solutions. Afr. J. Chem. Eng., 2013, 18, 70-76.

[5]. Singha B., Das S.K., Removal of Pb (II) ions from aqueous solution and industrial effluent using natural biosorbents. Environ. Sci. Pollut. R., 2012, 19, 2212-2226.

[6]. Hu J., Zhao D., Wang X., Removal of Pb (II) and Cu (II) from aqueous solution using multiwalled carbon nanotubes/iron oxide magnetic composites. Water Sci. Technol., 2011, 63, 917-923.

[7]. Dong L., Zhu Z., Qiu Y., Zhao J., Removal of lead from aqueous solution by hydroxyapatite/magnetite composite adsorbent. Chem. Eng. J., 2010, 165, 827-834.

[8]. Kara İ, Yilmazer D, Akar ST (2017) Metakaolin based geopolymer as an effective adsorbent for adsorption of zinc (II) and nickel (II) ions from aqueous solutions. Appl Clay Sci 139:54–63
[9]. Qiu R, Cheng F, Huang H (2018) Removal of Cd from aqueous solution using hydrothermally modified circulating fluidized bed fly ash resulting from coal gangue power plant. J Clean Prod 172:1918–1927
[10]. Horst MF, Alvarez M, Lassalle VL (2016) Removal of heavy metals from wastewater using magnetic nanocomposites: analysis of the experimental conditions. Sep Sci Technol 51:550–563
[11]. Hua M et al (2012) Heavy metal removal from water/wastewater by nanosized metal oxides: a review. J Hazard Mater 211(15):317–331
[12]. Warner CL, Chouyyok W, Mackie KE, Neiner D, Saraf LV, Droubay TC, Warner MG, Addleman RS (2012) Manganese doping of magnetic iron oxide nanoparticles: tailoring surface reactivity for a regenerable heavy metal sorbent. Langmuir 28:3931–3937
[13]. Yan J, Khoo E, Sumboja A, Lee PS (2010) Facile coating of manganese oxide on tin oxide nanowires with high-performance capacitive behaviour. ACS Nano 4(7):4247–4255
[14]. D. Habibi, S. Kaamyabi, H. Hazarkhani, Chin. J. Catal. 2015, 36, 362
[15]. S. P. Rajendran, K. Sengodan, Hindawi J. Nanosci. 2017, 2017, 1
[16]. Langmuir I (1916) The constitution and fundamental properties of solids and liquids. Part I. Solids. J Am Chem Soc 38:2221–2295
[17]. Nuri OS, Irannajad M, Mehdilo A (2019) Reagent adsorption on modified mineral surfaces: isotherm, kinetic and thermodynamic aspects. J Mol Liq 291:111311
[18]. Li E, Liang H, Du Z, Li D, Cheng F (2016) Adsorption process of octadecyl amine hydrochloride on KCl crystal surface in various salt saturated solutions: kinetics, isotherm model and thermodynamics properties. J Mol Liq 221:949–953
[19]. Fuku X, Diallo A, Maaza M (2016) Nanoscaled electrocatalytic optically modulated ZnO nanoparticles through green process of Punica granatum L. and their antibacterial activities. Int J Electrochem.
[20]. Fuku X, Kaviyarasu K, Matinise N, Maaza M (2016) Punicalagin green functionalized Cu/Cu2O/ZnO/CuO nanocomposite for potential electrochemical transducer and catalyst. Nanoscale Res Lett 11(1):386.
[21]. Matinise N, Fuku XG, Kaviyarasu K et al (2017) ZnO nanoparticles via Moringa oleifera green synthesis: physical properties & mechanism of formation. Appl Surf Sci 406:339–347.
[22]. Jagriti Gupta P. A. Hassan and K. C. Barrick, Core-shell Fe3O4@ZnO nanoparticles for magnetic hyperthermia and bio-imaging applications, AIP Advances 11, 025207 (2021)
[23]. Naresh Kumar Sethy*, Zeenat Arif, Pradeep Kumar Mishra and Pradeep Kumar, Green synthesis of TiO2 nanoparticles from Syzygium

cumin extract for photo-catalytic removal of lead (Pb) in explosive industrial wastewater, Green Process Synth 2020; 9: 171–181

[24]. Saranya K.S., Padil V.V.T., Senan C., Pilankatta R., Saranya K., George B., et al., Green Synthesis of High Temperature Stable Anatase Titanium Dioxide Nanoparticles Using Gum Kondagogu: Characterization and Solar Driven Photocatalytic Degradation of Organic Dye. Nanomaterials-Basel, 2018, 8, 1002-1021.

[25]. Xu J, Han X, Liu H, Hu Y. Synthesis and optical properties of silver nanoparticles stabilized by gemini surfactant. Colloid Surf A. 2006; 273:179–83.

[26]. Kucharczyk K, Rybka JD, Hilgendorff M et al (2019) Composite spheres made of bioengineered spider silk and iron oxide nanoparticles for theranostics applications. PLoS ONE 14: e0219790.

[27]. N.N. Nassar, Kinetics, equilibrium and thermodynamic studies on the adsorptive removal of nickel, cadmium and cobalt from wastewater by superparamagnetic iron oxide nano adsorbents, Can. J. Chem. Eng. 90 (2012) 1231–1238. doi:10.1002/cjce.20613.

[28]. H. Shayesteh, A. Rahbar-kelishami, R. Norouzbeigi, Evaluation of natural and cationic surfactant modified pumice for congo red removal in batch mode: Kinetic, equilibrium, and thermodynamic studies, J. Mol. Liq. 221 (2016) 1–11.doi: 10.1016/j.molliq.2016.05.053.

[29]. R.D.C. Soltani, G.S. Khorramabadi, a. R. Khataee, S. Jorfi, Silica nano powders/alginate composite for adsorption of lead (II) ions in aqueous solutions, J. Taiwan Inst. Chem. Eng. 45 (2014) 973–980. doi: 10.1016/j.jtice.2013.09.014.

[30]. Z. Shu, S. Wang, Synthesis and Characterization of Magnetic Nanosized / Composite Particles, J. Nanometre. 2009 (2009) 1–5. doi:10.1155/2009/340217

[31]. N.N. Nassar, Rapid removal and recovery of Pb (II) from wastewater by magnetic nano adsorbents, J. Hazard. Mater. 184 (2010) 538–546.doi: 10.1016/j.jhazmat.2010.08.069.

[32]. D. Mehta, S. Mazumdar, S.K. Singh, Magnetic adsorbents for the treatment of water / wastewater -A review, J. Water Process Eng. 7 (2015) 244–265. doi: 10.1016/j.jwpe.2015.07.001

[33]. J. Chen, F. He, H. Zhang, X. Zhang, G. Zhang, G. Yuan, Novel core-shell structured Mn-Fe / MnO2 magnetic nanoparticles for enhanced Pb (II) removal from aqueous solution Novel core-shell structured Mn-Fe / MnO 2 magnetic nanoparticles for, (2014). doi:10.1021/ie502967a.

[34]. Z.M. Badruddoza, a. S.H. Tay, P.Y. Tan, K. Hidajat, M.S. Uddin, Carboxymethyl-β-cyclodextrin conjugated magnetic nanoparticles as nano adsorbents for removal of copper ions: Synthesis and adsorption studies, J. Hazard.Mater. 185 (2011) 1177–1186. doi: 10.1016/j.jhazmat.2010.10.029.